Proceedings of the 4th International Congress APMAS2014, April 24-27, 2014, Fethiye, Turkey

Nanostructured ATO Anodes Produced by RF Magnetron Sputtering for Li-Ion Batteries

O. Cevher*, U. Tocoglu, H. Akbulut
Sakarya University, Engineering Faculty, Department of Metallurgical and Materials Engineering, Esentepe Campus 54187, Turkey

In this study, the reversible capacities, as well as the cycling behavior, of crystalline antimony-doped tin oxide (ATO) films have been investigated. ATO films were deposited on Cr-coated stainless steel substrates by the RF magnetron sputtering technique, with antimony-doped tin oxide (SnO_2:Sb) target in a mixed oxygen/argon gas environment. The ATO films were deposited for 1.0 h in a mixture of Ar and O_2 environment with O_2/Ar ratio of 10/90, at sputtering power of 75 W, 100 W and 125 W RF. ATO films were examined by X-ray diffraction (XRD), field emission scanning electron microscopy (FESEM). The electrochemical properties of ATO anodes were studied using 2016-type coin cells assembled in an argon-filled glove box.

DOI: 10.12693/APhysPolA.127.1065
PACS: 61.72.uj, 81.15.Cd, 82.47.Aa

1. Introduction

The SnO_2 film is a transparent conductive coating material and a n-type semiconductor with a wide band gap (approximately 3.7 eV) [1] and tetragonal rutile structure. The SnO_2 film shows the best thermal and chemical stability, it is inexpensive, and it has good adhesion to most of the substrates, however it has a high resistivity. The optical band gap, resistivity, carrier type and concentration in SnO_2 films can be easily adjusted by doping with antimony (Sb), indium (In) and/or fluorine (F) [24].

The properties of the SnO_2 films are generally affected by preparation conditions such as deposition technique, substrate temperature, working pressure, type of substrates and the thickness of the film [5]. The SnO_2 films can be deposited by various techniques such as sputtering [6], pulsed laser deposition [7], chemical vapor deposition [8], thermal evaporation [9], spray pyrolysis [10], dip coating [11]. RF magnetron sputtering is one of the most promising deposition techniques due to the advantages of low deposition temperature, simple processing, inexpensive equipment and suitability for large area deposition, whilst yielding the preferred orientation and uniform properties [12].

The Li-ion battery industry is increasingly looking for materials with a higher capacity for lithium storage, than the currently used graphite anodes (372 mA h g^{-1}) [13], for use in the next generation of more powerful rechargeable batteries. Tin is one of the best solutions available, due to its high theoretical capacity (1494 mA h g^{-1}) [14] and other technical benefits. However, its practical use is hampered by a poor cyclability, which is caused by the mechanical damage of the electrodes, due to the large volume change (ca. 300%) and Li_2O formation during charging and discharging processes [15–17]. Many efforts have been devoted to attempt to reduce the capacity fading.

In this work, the effect of RF power on the electrochemical characteristics of ATO as anode material was investigated.

2. Experimental

The ATO thin films were deposited on silicon wafer and Cr-coated stainless steel substrates using RF magnetron sputtering. As a target was used a SnO_2:Sb disc (SnO_2:Sb=90:10 wt.%, purity of 99.99%) with a diameter of 50.8 and thickness of 6.35 mm. The applied RF power was 75 W, 100 W and 125 W. The crystalline structure of ATO thin films was characterized by X-ray diffraction (XRD) technique. The XRD patterns of the deposited ATO thin films were obtained by an X-ray diffractometer (Rigaku D/MAX 2000 with a multipurpose attachment) using Cu K_α radiation ($\lambda = 1.54056$ Å). The grain size was calculated by Scherrer's formula [18]:

$$D = \frac{0.9\lambda}{B\cos\theta}, \tag{1}$$

where D is the mean grain size, λ is the X-ray wavelength, B is the corrected full-width at half maximum (FWHM) and θ is the Bragg angle. The surface morphology of ATO thin films was investigated by field emission scanning electron microscopy (FESEM) (JSM-6335F). Coin-type (CR2016) test cells were assembled in an argon-filled glove box, directly using ATO coated stainless steel substrates as the working electrode. The cells were aged for 12 h before measurements. The cells were cyclically tested on a MTI BST8-MA Battery Analyzer using different current densities, over a voltage range of 0.05–3.0 V. The charge/discharge behaviour of the cells was measured galvanostatically at a charge/discharge rate of 1 C in the 0.05 V to 3.0 V range.

*corresponding author; e-mail: ocevher@sakarya.edu.tr

3. Results and discussions

FESEM micrographs of the ATO thin films deposited on silicon wafer, using various RF power values, at oxygen partial pressure of 10%, are presented in Fig. 1a, 1b and 1c. The ATO thin films have a relatively smooth and dense surface. Grain agglomerates are also observed. The results show that the ATO thin films are made of nano-sized particles. The grain size increases gradually with the RF power. When the RF power is about 75 W, the average particle size is about 8.9 nm (Fig. 1a), when RF power is increased to 125 W, the grains also increase to about 13.6 nm (Fig. 1c). From this result, the grain size was observed to get bigger with the increase in the RF power, because the increased power had caused an increase in the energy of the Ar^+ ions, when they collided with the target, and then an increase in the surface mobility of the sputtered particles [12].

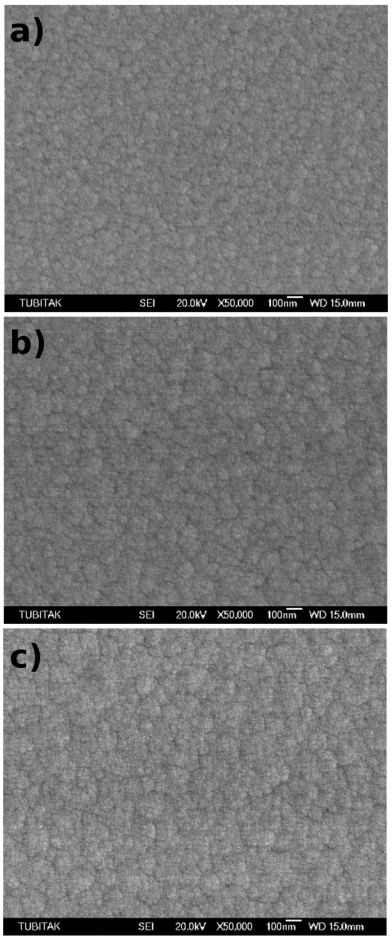

Fig. 1. FESEM micrographs of the ATO thin films deposited at partial oxygen pressure of 10%, and RF power value of a) 75 W, b) 100 W and c) 125 W.

The crystallographic structure of ATO thin films deposited at various RF power values at oxygen partial pressure of 10% was characterized by X-ray diffraction and the results are presented in Fig. 2. The diffraction peaks indicate that tin oxide exists in cassiterite tetragonal (rutile type) structure (JCPDS card number 00-041-1445). The (110), (101) and (211) diffraction peaks were observed for ATO thin films deposited at various values of RF power, at oxygen partial pressure of 10%. The peaks become more intense and sharper with the increase in RF power. This suggests that the crystallinity of the resulting film increases and the grain size becomes larger with increasing RF power (under the oxide region of the Shinoki model [19], where the crystallinity was enhanced with increasing RF power) [20, 21].

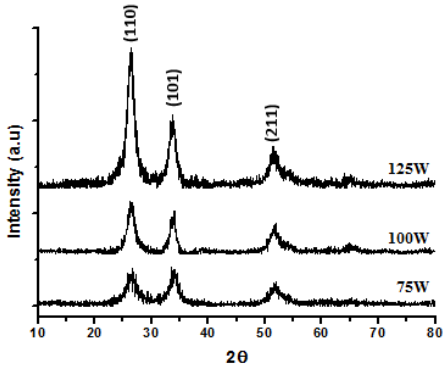

Fig. 2. X-ray diffraction patterns of the ATO thin films deposited at different values of RF power, at oxygen partial pressure of 10%.

The discharge-charge curves of ATO anode materials during the 50th cycle, at a constant current of 1.0 C, are shown in Fig. 3a, 3b and 3c. As shown in Fig. 3a, the discharge and charge capacities of the 1st cycle are 1423 mA h g^{-1} and 936 mA h g^{-1}, respectively, which indicates that its coulombic efficiency is 65%. As shown in Fig. 3b, the discharge and charge capacities of the 1st cycle are 1472 mA h g^{-1} and 971 mA h g^{-1}, respectively, which indicates that its coulombic efficiency is 65%. As shown in Fig. 3c, the discharge and charge capacities of the 1st cycle are 1493 mA h g^{-1} and 1007 mA h g^{-1}, respectively, which indicates that its coulombic efficiency is 67%. There is a large irreversible capacity in the 1st cycle in all ATO anode materials, which can be attributed to formation of solid-electrolyte interface (SEI) and decomposition of electrolyte at a low voltage [22].

Figure 4 shows the curves of discharge capacity versus cycle number for ATO anode materials. As can be seen from Fig. 4, the discharge capacities of the anode materials at RF power of 75 W, 100 W and 125 W and the at 50th cycle are approximately 165 mA h g^{-1}, 295 mA h g^{-1} and 317 mA h g^{-1}, respectively. During the 50th cycle, the SnO_2:Sb anode material, deposited at RF power of 125 W, has a high discharge capacity of 317 mA h g^{-1}, due to crystallinity of the ATO anode, which is better than that of other the ATO anodes.

4. Conclusions

ATO films were deposited on Cr-coated stainless steel

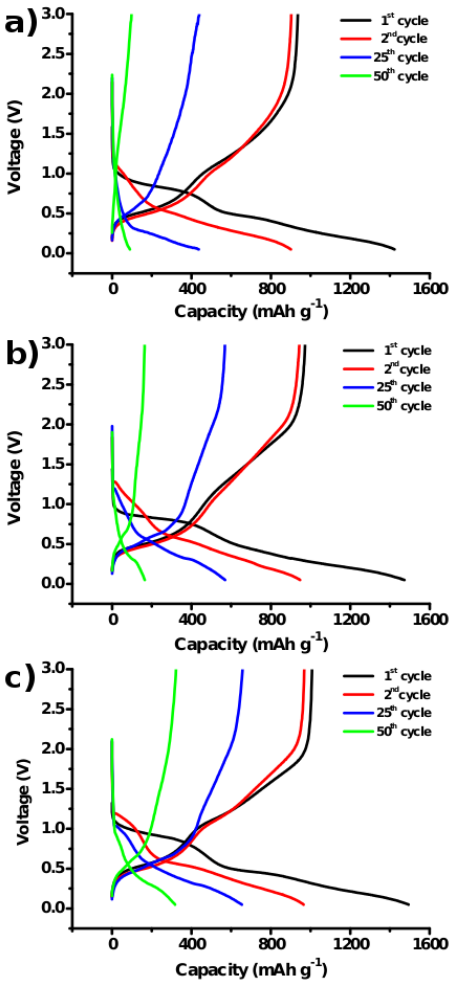

Fig. 3. Discharge capacity for ATO anode materials produced at different values of RF power, a) 75 W, b) 100 W and c) 125 W.

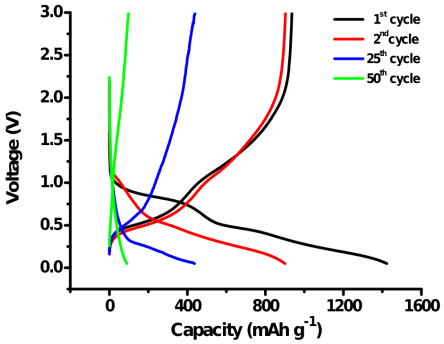

Fig. 4. Comparison of the cycling performance for ATO anode materials produced at different values of RF power, at oxygen partial pressure of 10%.

substrates by RF magnetron sputtering technique in a mixture of Ar and O_2 environment with O_2/Ar ratio of 10/90 wt.% at RF sputtering power of 75 W, 100 W and 125 W. XRD peaks become more intense and sharper with the increase in RF power. The mean grain size increases with the increase of the RF power. The best electrochemical results were obtained with ATO anode produced at RF power of 125 W (317 mA h g^{-1}) in highest 50 cycles discharge capacity.

Acknowledgments

This work is supported by the Scientific and Technological Research Council of Turkey (TUBITAK). The authors thank the TUBITAK MAG workers for their financial support.

References

[1] F.J. Arlinghaus, *J. Phys. Chem. Solids* **35**, 931 (1974).

[2] K.Y. Rajpure, M.N. Kusumade, M.N. Neumann-Spallart, C.H. Bhosale, *Mater. Chem. Phys.* **64**, 184 (2000).

[3] T. Kawabe, S. Shimomura, T. Karasuda, K. Tabata, E. Suzuki, Y. Yamaguchi, *Surf. Sci.* **448**, 101 (2000).

[4] K.L. Chopra, S. Major, D.K. Pandya, *Thin Solid Films* **102**, 1 (1983).

[5] L.P. Peng, L. Fang, X.F. Yang, H.B. Ruan, Y.J. Li, Q.L. Huang, C.Y. Kong, *Physica E* **41**, 1819 (2009).

[6] B. Stjerna, E. Olsson, C.G. Granqvist, *J. Appl. Phys.* **76**, 3797 (1994).

[7] N.H. Hong, N. Poirot, J. Sakai, *Phys. Rev. B* **77**, 033205 (2008).

[8] G. Sanon, R. Rup, A. Mansingh, *Phys. Rev. B* **44**, 5672 (1991).

[9] J. Wu, K. Yu, L. Li, J.W. Xu, D.J. Shang, Y.E. Xu, ZQ. Zhu, *J. Phys. D: Appl. Phys.* **41**, 185302 (2008).

[10] M.B. Mohagheghi, M.S. Saremi, *Physica B* **405**, 4205 (2010).

[11] S.S. Park, J.D. Mackenize, *Thin Solid Films* **258**, 268 (1995).

[12] S.U. Lee, J.H. Boo, B. Hong, *Jpn. J. Appl. Phys* **50**, 01AB10 (2011).

[13] H. Buqa, D. Goers, M. Holzapfel, M.E. Spahr, P. Novak, *J. Electrochem. Soc.* **152**, A474 (2005).

[14] W.F. Liu, X.J. Huang, Z.X. Wang, H. Li, L. Chen *J. Electrochem. Soc.* **145**, 59 (1998).

[15] N. Li, C.R. Martin, *J. Electrochem. Soc.* **148**, A164 (2001).

[16] S. Han, B. Jang, T. Kim, S.M. Oh, T. Hyeon, *Adv. Funct. Mater.* **15**, 1845 (2005).

[17] J. Fan, T. Wang, C. Yu, B. Tu, Z. Jiang, D. Zhao, *Adv. Mater.* **16**, 1432 (2004).

[18] B.D. Cullity, *Elements of X-Ray Diffraction*, Addison-Wesley, Massachusetts 1956.

[19] F. Shinoki, A. Itoh, *J. Appl. Phys.* **46**, 3381 (1975).

[20] S.M. Chou, L.G. Teoh, W.H. Lai, Y.H. Su, M.H. Hon, *Sensors* **6**, 1420 (2006).

[21] C. Lee, K. Kim, K. Prabakar, *J. Korean Phys.Soc.* **48**, 1193 (2006).

[22] J.M. Ma, J.Q. Yang, L.F. Jiao, Y.H. Mao, T.H. Wang, X.C. Duan, J.B. Lian, W.J. Zheng, *Cryst. Eng. Comm.* **14**, 453 (2012).